JGS
Journal of the Geological Society

Research article

Published online November 10, 2015 doi:10.1144/jgs2015-071 | Vol. 173 | 2016 | pp. 282–291

An example of low-Th/U zircon overgrowths of magmatic origin in a late orogenic Variscan intrusion: the San Ciprián massif (NW Spain)

Marco A. Lopez-Sanchez[1*], John N. Aleinikoff[2], Alberto Marcos[1], Francisco J. Martínez[3] & Sergio Llana-Fúnez[1]

[1] Geology Department, University of Oviedo, 33005 Oviedo, Spain
[2] US Geological Survey, Denver, CO 80225, USA
[3] Geology Department, Autonomous University of Barcelona, 08193 Barcelona, Spain
* Correspondence: malopez@geol.uniovi.es

Abstract: Th/U values in zircon are commonly used to discriminate between metamorphic (Th/U < 0.1) and magmatic (Th/U > 0.1) origin for zircon overgrowths. We test this hypothesis in the San Ciprián massif, a late orogenic granitic intrusion in the hinterland of the Variscan orogeny. Zircon grains from this granite have cores with inherited Ediacaran ages and Th/U > 0.1, whereas zircon mantles yield an age of about 287 Ma, interpreted as the time of crystallization of the granite, and have Th/U < 0.1. Hence, the San Ciprián massif presents an uncommon but unambiguous example of magmatic zircon mantles with Th/U values typical of metamorphic zircon. The most likely causes for the unusually low-Th/U zircon values in the San Ciprián massif are a combination of a U-rich magma composition (owing to a fractionation process) and the absence of other U-enriched accessory minerals. Our work in determining Th/U ratios substantiates the warning previously made by some researchers and precludes the use of Th/U values in zircon as an unequivocal indicator of metamorphic origin in the absence of other chemical, zircon morphology or field-based independent criteria.

Supplementary materials: Code and data to generate Figures 1 and 5 are available at http://www.geolsoc.org.uk/SUP18885.

Received 5 June 2015; **revised** 5 September 2015; **accepted** 7 September 2015

Zircon is of singular importance in Earth science (Harley & Kelly 2007), given its ubiquity in most rock types, and particularly owing to its resistance to the effects of various crustal processes. Zircon is extremely useful in petrological studies, both as a geochronometer (U–Pb method) and as an indicator of source rock type (via trace element content). A commonly employed criterion to discriminate between magmatic and metamorphic zircon is the Th/U ratio (Williams & Claesson 1987; Hoskin & Black 2000; Rubatto 2002), where Th/U > 0.1 usually indicates a magmatic origin whereas Th/U < 0.1 usually indicates a metamorphic origin (Fig. 1a). This threshold of Th/U at 0.1 has been set empirically based on observations in natural rocks, and it has received considerable attention in the past 35 years. Hypotheses explaining the causes of Th/U variability include partitioning behaviour of Th and U between zircon and coexisting minerals (e.g. Ahrens *et al.* 1967; Hokada & Harley 2004), change in the growth mechanism in zircon owing to varying environmental factors (e.g. Vavra *et al.* 1999), differential expulsion of Th and U during zircon recrystallization (e.g. Hoskin & Black 2000), speed of crystal growth (Watson 1996) and element availability in partial melts (e.g. Belousova *et al.* 2002; Rubatto 2002). Also, it was found that the Th/U ratio in zircon changes with temperature. For example, zircon Th/U increases with temperature under equilibrium conditions (Watson & Harrison 1983) but, in contrast, zircon Th/U decreases with temperature in the case of melt fractionation processes (Claiborne *et al*. 2010; Kirkland *et al*. 2015).

The use of Th/U ratio to discriminate between igneous and metamorphic origins has recently been questioned (Harley *et al*. 2007) because there are examples reported in the literature in which metamorphic zircon overgrowths have Th/U values of greater than 0.1 or have highly variable values (Fig. 1b), particularly in high-grade environments (Pidgeon 1992; Schaltegger *et al.* 1999; Vavra *et al.* 1999; Möller *et al.* 2003; Hokada & Harley 2004; Kelly & Harley 2005; Wang *et al*. 2011). In contrast, most Th/U values in magmatic zircons are above 0.5 (e.g. Belousova *et al*. 2002; Kirkland *et al*. 2015). Although magmatic zircons with Th/U values below 0.1 have been found (e.g. Schärer 1984; Sláma *et al*. 2008), examples of zircon mantles or rims interpreted as magmatic overgrowths with Th/U values below 0.1 are rare in the literature (Zeck & Whitehouse 1999; Ladenberger *et al*. 2013).

The San Ciprián massif is a leucogranitic pluton located in the NW part of the Iberian Variscan massif within the Lugo Dome (Spain) (Fig. 2a and b; Capdevila 1969). During a U–Pb dating study of zircon from San Ciprián-related granite dykes by the laser ablation inductively coupled plasma mass spectrometry (LA-ICP-MS) technique (Lopez-Sanchez *et al*. 2015), cathodoluminescence (CL) imagery revealed that nearly all of the zircon grains are composed of Ediacaran or Early Cambrian bright inner cores and Permian dark-zoned mantles. Cores have Th/U values greater than 0.1 and dark-zoned mantles have Th/U below 0.1. The relative age of San Ciprián granite emplacement with respect to other dated igneous rocks and regional deformation is fairly well established (Bastida *et al.* 1986; Galán 1987). Cross-cutting relationships between the San Ciprián massif and its host rocks, including some older igneous rocks, indicate that the Permian dark-zoned mantles must be magmatic (see below for details). In this study, zircon grains enclosed within the San Ciprián massif are analysed using a sensitive high-resolution ion microprobe (SHRIMP) to determine the chemistry of cores and rims for comparison with zircons within the granite dykes. The potential underlying processes producing low Th/U are discussed in the light of our results and in the context of published ratios of various igneous rocks with emphasis on peraluminous granitic rocks.

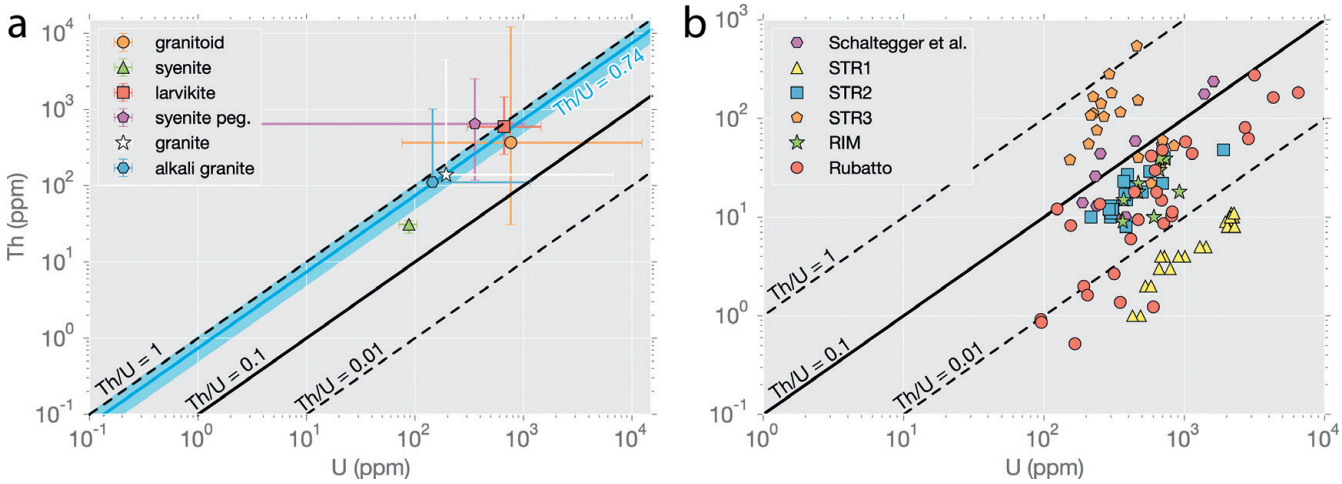

Fig. 1. (**a**) Typical Th v. U content in igneous zircons belonging to various igneous rock types from Belousova *et al*. (2002) and Kirkland *et al*. (2015). Points represent the median or the Tukey's biweight robust mean of all values and error bars show the range of values obtained. For reference, the dark grey (blue online) shaded band represents the most typical values (the interquartile range) of Th/U zircon values obtained from a population of 1963 granites; the line inside this band is the Tukey's biweight robust mean reported by Kirkland *et al*. (2015). (**b**) Typical Th v. U content in metamorphic zircons belonging to various metamorphic environments, from amphibolite to granulite facies (Schaltegger *et al*. 1999; Vavra *et al*. 1999; Rubatto 2002).

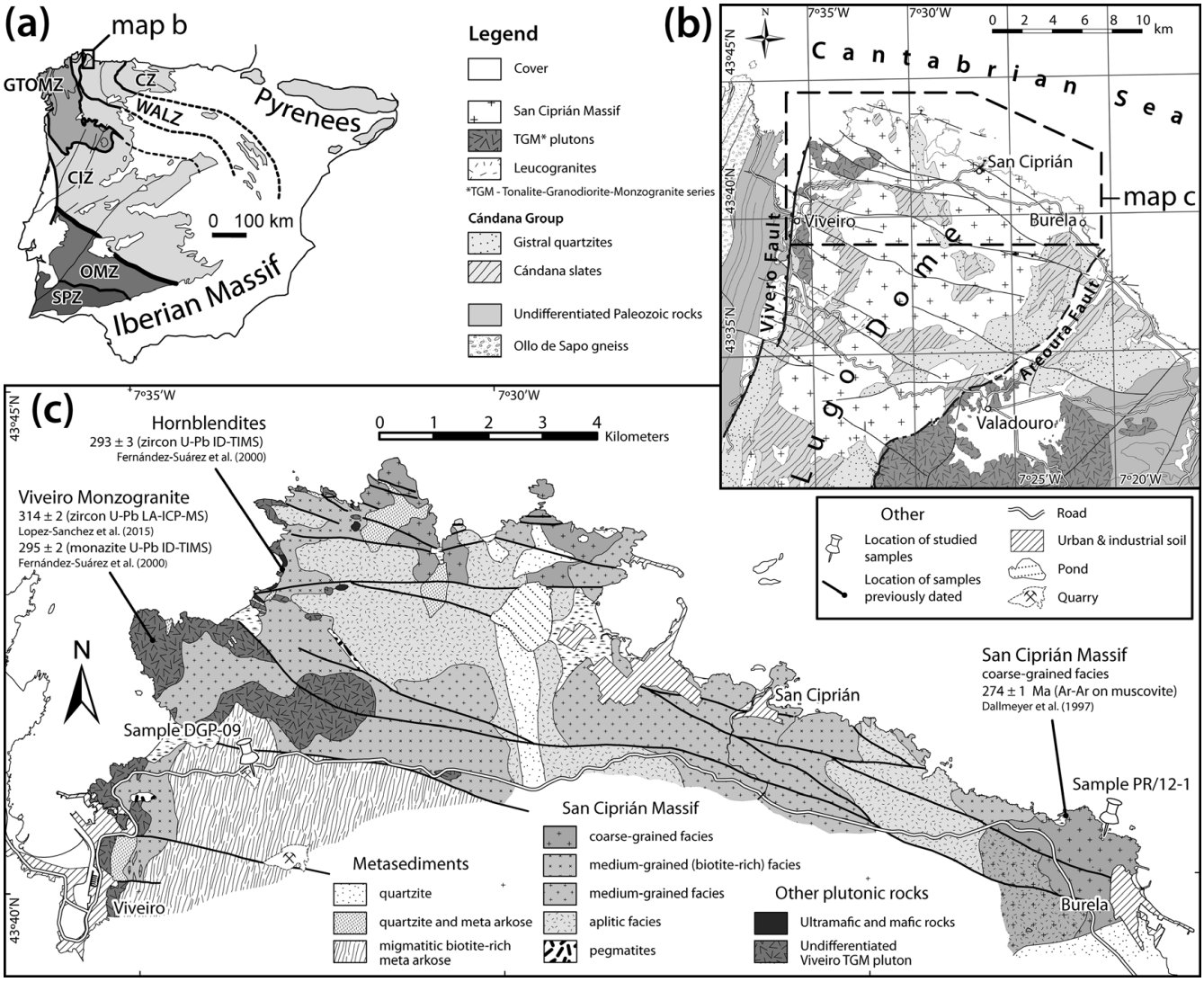

Fig. 2. (**a**) Map of the Iberian Peninsula showing the zones of the Iberian massif: CZ, Cantabrian Zone; WALZ, West Asturian–Leonese Zone; GTOMZ, Galicia Tras-Os-Montes Zone; CIZ, Central Iberian Zone; OMZ, Ossa Morena Zone; SPZ, South Portuguese Zone (Lotze 1945; Julivert *et al.* 1972; Farias *et al.* 1987). (**b**) Simplified geological map of the northern part of the Lugo Dome within the West Asturian–Leonese Zone showing the location of the San Ciprián massif (based on Lopez-Sanchez 2013 and Marcos 2013). (**c**) Local map of the northern part of the San Ciprián massif showing the facies of the pluton (redrawn from Galán 1987). The location of the studied samples and other previous samples of interest for the study are indicated.

Geological features and previous data on the age of the San Ciprián massif

The San Ciprián massif is a strongly peraluminous, low-Ca granite (silica content 72–76%) composed of quartz, plagioclase ($An_{30–00}$), K-feldspar, biotite and muscovite. Accessory minerals include zircon, apatite, monazite and opaque minerals (Galán 1987; Fernández-Suárez *et al.* 2000). On the basis of grain size and the chemical composition of biotite and muscovite, four facies, ranging from alkali feldspar granite to monzogranite, are distinguished (Galán 1987; Fig. 2c): (1) a medium-grained facies mostly with biotite (5.7%); (2) a medium-grained facies with biotite (3.9%) and muscovite (2.7%); (3) a coarse-grained facies with biotite (2.1%) and muscovite (6.6%); (4) an aplitic facies mainly with muscovite (8.2%) (biotite <2.5%). The medium-grained facies are essentially monzogranites, the coarse-grained facies varies between alkali feldspar granite and monzogranite, and the aplitic facies is an alkali feldspar granite (Galán 1987).

Host-rock and regional structure relations

The San Ciprián massif was emplaced into Cambrian metasedimentary rocks and occurs as a stratiform, flat-lying, sub-concordant body within the host metamorphic rocks (Marcos 2013). The pluton clearly cuts a tectonic foliation and folds related to the main Variscan deformation, which is Devonian or younger in the northwestern part of the Iberian Peninsula (Dallmeyer *et al*. 1997). Exposures of granite indicate that both host-rock lithology and structure (i.e. primary and tectonic foliations) controlled emplacement. Quartzite xenoliths that occur within the granite originated as metapsammitic units of the Candana Group. Metamorphic host rocks contain sillimanite or andalusite related to the intrusion of granitic bodies; some of the host rocks have undergone partial migmatization (Capdevila 1969; Bastida *et al.* 1984). Andalusite porphyroblasts sporadically include remnants of staurolite and garnet. The pluton is in part bounded to the west by a north–south crustal-scale extensional shear zone, the Vivero fault, with a top-to-the-west sense of shear (Fig. 2b and c; Martínez-Catalán 1985; Martínez *et al.* 1996; Lopez-Sanchez 2013; Lopez-Sanchez *et al*. 2015). To the east, the pluton is partially bounded by a low-dipping shear zone (recently renamed as the Areoura fault; Marcos 2013) with top-to-the-east sense of shear (Fig. 2b). Most of the pluton shows no evidence of solid-state deformation, although Galán (1987) reported some local flat-lying metre-scale shear zones throughout the massif. In contrast, in its western margin, the pluton has an intensely deformed solid-state fabric with a WNW–ESE mineral lineation that Bastida *et al.* (1986) related to the development of the Vivero (normal) fault.

In the northwestern part of the San Ciprián massif (Fig. 2c), the medium-grained facies cuts, and contains enclaves of, calc-alkaline granitoids belonging to the Vivero pluton and a small volume of peridotites, pyroxenites and hornblendites (Galán 1987; Galán *et al.* 1996). The emplacement age of the Vivero pluton was recently determined to be 314 ± 2 Ma (zircon U–Pb LA-ICP-MS; Lopez-Sanchez 2013; Lopez-Sanchez *et al*. 2015). Ultramafic rocks, specifically the hornblendites, were interpreted as having been emplaced at 293 ± 3 Ma (zircon upper-intercept U–Pb isotope dilution thermal ionization mass spectrometry (ID-TIMS); Fernández-Suárez *et al.* 2000). Hence, the Permian age obtained within the ultramafic rocks sets an older limit to the San Ciprián massif emplacement age, at least for the medium-grained facies.

The San Ciprián massif is cut by a number of discrete subvertical brittle faults that generally trend WNW–ESE (Fig. 2b and c). Their orientations are similar to the As Pontes fault located farther south, a well-constrained Alpine-age structure affecting a Cenozoic basin (Ferrus-Piñol 1994; Huertas *et al.* 1997).

Previous data on the age of the San Ciprián massif

Early attempts to determine the crystallization age of the San Ciprián massif include (1) whole-rock Rb–Sr analysis yielding an age of 287 ± 7 Ma (MSWD = 0.52) (Bellido *et al.* 1992) and (2) a U–Pb ID-TIMS age based on two slightly reverse discordant monazite analyses that yielded a ^{207}Pb–^{235}U age of 286 ± 2 Ma (Fernández-Suárez *et al.* 2000). An attempt to date this pluton using zircon multi-grain ID-TIMS analyses (Fernández-Suárez *et al.* 2000) resulted in highly discordant data points owing to the presence of major inherited components. An Ar/Ar age on muscovite from within the coarse-grained facies of the San Ciprián massif yielded a plateau age of 274 ± 1 Ma (Dallmeyer *et al.* 1997), thought to represent cooling through about 400°C. Lopez-Sanchez *et al*. (2015) determined a zircon LA-ICP-MS U–Pb age of 287 ± 3 Ma (MSWD = 0.89, probability of fit = 0.45), for a deformed granite dyke, which coincides with the Early Permian (Artinskian) age previously obtained using other dating methods. More importantly, the CL imagery from that study also revealed that nearly all zircons show bright Ediacaran–Early Cambrian cores and dark-zoned Permian mantles; the inherited cores have Th/U values greater than 0.1 and the dark mantles have Th/U of less than 0.1.

Samples and methods

About 5 kg of sample PR12-1 was collected at Ril beach located about 1 km north of Burela town (43°40′17.99″N, 7°21′53.26″W). This sample is a fresh, medium- to coarse-grained undeformed leucogranite. It is located near the eastern boundary of the San Ciprián granite and 730 m from the location of the Ar/Ar muscovite sample previously dated by Dallmeyer *et al.* (1997) (Fig. 2c). Sample DGP-09 (Lopez-Sanchez *et al*. 2015) was collected in a quarry (near the N-642 road) located about 3.7 km NE of Viveiro (43°41′06.45″N, 7°33′29.85″W) (Fig. 2c). This sample was collected from a fresh, medium-grained granite dyke with a variable thickness of about 30–50 cm. The leucocratic dyke cuts the gneissic foliation of the host rocks and is folded. The dyke appears to be a medium-grained facies of the San Ciprián massif.

Analytical methods: SHRIMP-RG dating

Zircon was extracted from sample PR12-1 using conventional mineral separation methods at the US Geological Survey in Denver, CO. Zircon standard R33 (419 Ma; Black *et al*. 2004) plus grains from PR12-1 were mounted in epoxy, ground to nearly half thickness and polished with 6 µm and 1 µm grit diamond suspension abrasive. Transmitted- and reflected-light images were taken of all mounted zircon grains. In addition, all mounted grains were imaged in CL using a scanning electron microscope.

Zircon from sample PR12-1 was dated following the methods of Williams (1998) using the USGS–Stanford sensitive high-resolution ion microprobe-reverse geometry (SHRIMP-RG) at Stanford University. The primary ion beam was about 20–25 µm in diameter. For each analysis, the magnet was cycled through the appropriate mass stations five times. SHRIMP data for zircon were reduced using Squid 2 (Ludwig 2009) and plotted using Isoplot 3 (Ludwig 2012). Concentrations of U and Th are believed to be accurate to about ±20% (Ireland 1995), and are used only for comparing analyses. U–Pb age data for zircon from the San Ciprián granite are shown on a Tera–Wasserburg plot; the SHRIMP age is calculated using the weighted average of selected $^{206}Pb/^{238}U$ data.

Details on analytical method (LA-ICP-MS U(Th)–Pb) used to date sample DGP-09 have been given by Lopez-Sanchez *et al*. (2015).

Whole-rock major and trace element geochemistry

Granite samples DGP-09 and PR12-1 were crushed and milled to very fine powder in a tungsten carbide cup. Whole-rock powders were analysed for major elements by energy-dispersive X-ray fluorescence (XRF) analysis on fused glass discs at the University of Oviedo. Uncertainties in major elements are bracketed between 1 and 3% relative. Trace elements were determined on pressed powder pellets by energy-dispersive XRF at the University of Oviedo and for comparison by fusion-inductively coupled plasma mass spectrometry (FUS-ICP-MS) at Activation Laboratories Limited (ACTLABS), Ontario, Canada. Uncertainties in U and Th are bracketed for most elements between 1 and 2 ppm for XRF and 0.01 and 0.05 ppm for ACTLABS FUS-ICP-MS. More information on procedure, precision and accuracy of FUS-ICP-MS can be found at www.actlabs.com.

Results

CL images from both samples show that zircon grains are euhedral, displaying doubly terminated prismatic shapes (Fig. 3; Lopez-Sanchez *et al*. 2015). Almost all grains show bright cores displaying concentric oscillatory zoning and dark-zoned mantles. In some cases, the mantles cut growth zoning of cores, implying the operation of dissolution and re-precipitation processes during their formation. Some of the zircons from the coarse-grained facies of the granite (sample PR12-1) also show thin unzoned dark rims overgrowing the dark-zoned mantles (Fig. 3).

For sample PR12-1, a total of 17 SHRIMP measurements were performed, four in the bright oscillatory-zoned cores, eight in the dark-zoned mantles, and five in the dark unzoned tips. The bright inner cores yielded Tonian (994 Ma), Ediacaran (599 and 580 Ma) and Late Cambrian (506 Ma) ages (Fig. 4). The uranium and thorium contents of the bright cores are between 244 and 717 ppm (average 404 ppm) and 71 and 216 ppm (average 157 ppm), respectively (Tables 1 and 2). Th/U ratios in cores range from about 0.25 to 0.88 (Fig. 5a; Table 2). The dark-zoned mantles show uranium content between 801 and 2426 ppm (average 1524 ppm) and thorium content between 17 and 117 ppm (average 59 ppm). Th/U ratios are between 0.014 and 0.123, slightly lower, although similar to those found within zircon from sample DGP-09 (Lopez-Sanchez *et al*. 2015). Seven SHRIMP analyses of dark-zoned mantles yielded a weighted average age of 286.5 ± 3.1 Ma (2σ, MSWD = 0.57; Fig. 4), similar to the age obtained in the dark-zoned mantles of sample DGP-09. The dark unzoned tips have the highest uranium content, up to 7166 ppm (average 4228 ppm), and Th/U ratios between 0.001 and 0.043 (Tables 1 and 2). They yielded scattered ages, from 326 to 260 Ma (Fig. 4; Table 2), and do not produce a coherent weighted average age; four analyses have older $^{206}Pb/^{238}U$ than the dark-zoned mantles, probably an analytical artefact owing to matrix effects caused by high U content (Williams & Hergt 2000; White & Ireland 2012). As a result, the dark unzoned tips were not considered further.

For comparison, zircons from granite dyke sample DGP-09 are composed of bright oscillatory-zoned cores that contain 173–741 ppm U (average 350 ppm) and 56–217 ppm Th (average 126 ppm), and have Th/U ratios between 0.24 and 0.46 (average 0.33). These cores yield ages of 585–548 Ma and are interpreted as inherited grains. In contrast, the U and Th contents in the dark-zoned mantles are between 1729 and 3175 ppm and 45 and 127 ppm, respectively; the Th/U ratios vary between 0.02 and 0.04 (Fig. 5a). Three dark-zoned mantles yielded a weighted average age of 287 ± 2 Ma (95% confidence, MSWD = 0.58, probability of fit = 0.56; Lopez-Sanchez *et al*. 2015).

Whole-rock analysis of U and Th using two techniques yielded similar values within error in the same samples (Table 3). The obtained Th/U whole-rock ratios are 0.77 (DGP-09) and 2.08 (PR12-1), respectively.

Discussion and conclusions

The crystallization age of the San Ciprián massif is now firmly established at 287 ± 3 Ma. This age is supported by several techniques (concordant zircon U–Pb, concordant monazite U–Pb, whole-rock Rb–Sr) and falls within the current analytical uncertainties for the techniques involved in samples collected from different places and facies throughout the massif, suggesting that the pluton was formed by a single magmatic event. This age confirms that the San Ciprián massif is the youngest Permian pluton in the northwestern Iberian massif.

CL imagery shows complex patterns in zircon within the San Ciprián massif: bright inner cores, high-U dark-zoned mantles and dark unzoned rims. On the basis of crosscutting relationships with the host rocks (which contain a Variscan tectonic foliation) and several Carboniferous igneous rocks, the cores are interpreted as inherited. Consequently, the dark-zoned mantles are interpreted as magmatic in origin. This is an unambiguous example of zircon magmatic overgrowths with Th/U < 0.1 (Fig. 5a). This finding puts more constraints on the use of this empirical threshold ratio as a discriminant of zircon overgrowth origin solely on the basis of this value. Although most magmatic zircons have Th/U values greater than 0.1, our example shows that is not universally true, and therefore our results substantiate the cautionary notes of Harley *et al.* (2007). This finding is especially critical for studies that attempt to unravel geological histories of zircons within sediments based only on Th/U ratios and SEM-CL images. Thus, if detrital zircon derived from the San Ciprián massif were dated as part of a provenance study, the data could be misinterpreted to indicate 'magmatic' cores and 'metamorphic' overgrowths, and therefore the younger age would suggest a 'metamorphic' event.

Figure 5a shows that the Th content in the dark-zoned mantles, although slightly lower, is rather similar to that obtained in the bright zircon cores. In contrast, the U content in the dark-zoned mantles is significantly higher than that observed in the bright zircon cores. Considering the range of Th and U values obtained in zircons belonging to various granites (Belousova *et al*. 2002; Kirkland *et al*. 2015), the U and Th values obtained in the zircon overgrowths belonging to the San Ciprián massif are within the typical range, although far from the most common values. Furthermore, although the low Th/U is unusual in magmatic zircons, similar values have been reported occasionally in zircons belonging to high-SiO_2 and/or peraluminous granites (Table 4; Fig. 5b).

Comparing the plots shown in Figures 1b and 5b, it seems that the Th/U together with the U content cannot be used to discriminate between 'metamorphic' and 'magmatic' zircons. In contrast, zircons with very low Th values (<5 ppm) are rare in magmatic zircon (Fig. 5b), but are common in metamorphic zircon (Fig. 1b). This suggests that the Th content of zircon, together with the Th/U, might be a useful discriminant for zircon origin in very specific cases. In any event, given the small amount of data available showing magmatic zircons with Th/U < 0.1, this suggestion should be taken with care and further study is needed.

Based on the U and Th data, additional interesting questions arise. (1) What are the possible causes for the magmatic zircon overgrowths of the San Ciprián massif that have low Th/U values typical of metamorphic zircons? (2) Are these uncommon Th/U ratios related to abnormal Th/U in the magma? (3) Why is there a high proportion of inherited cores within the San Ciprián massif?

Whole-rock analyses of PR12-1 and DGP-09 yielded Th/U ratios of 2.08 and 0.77, respectively. Because inherited zircon

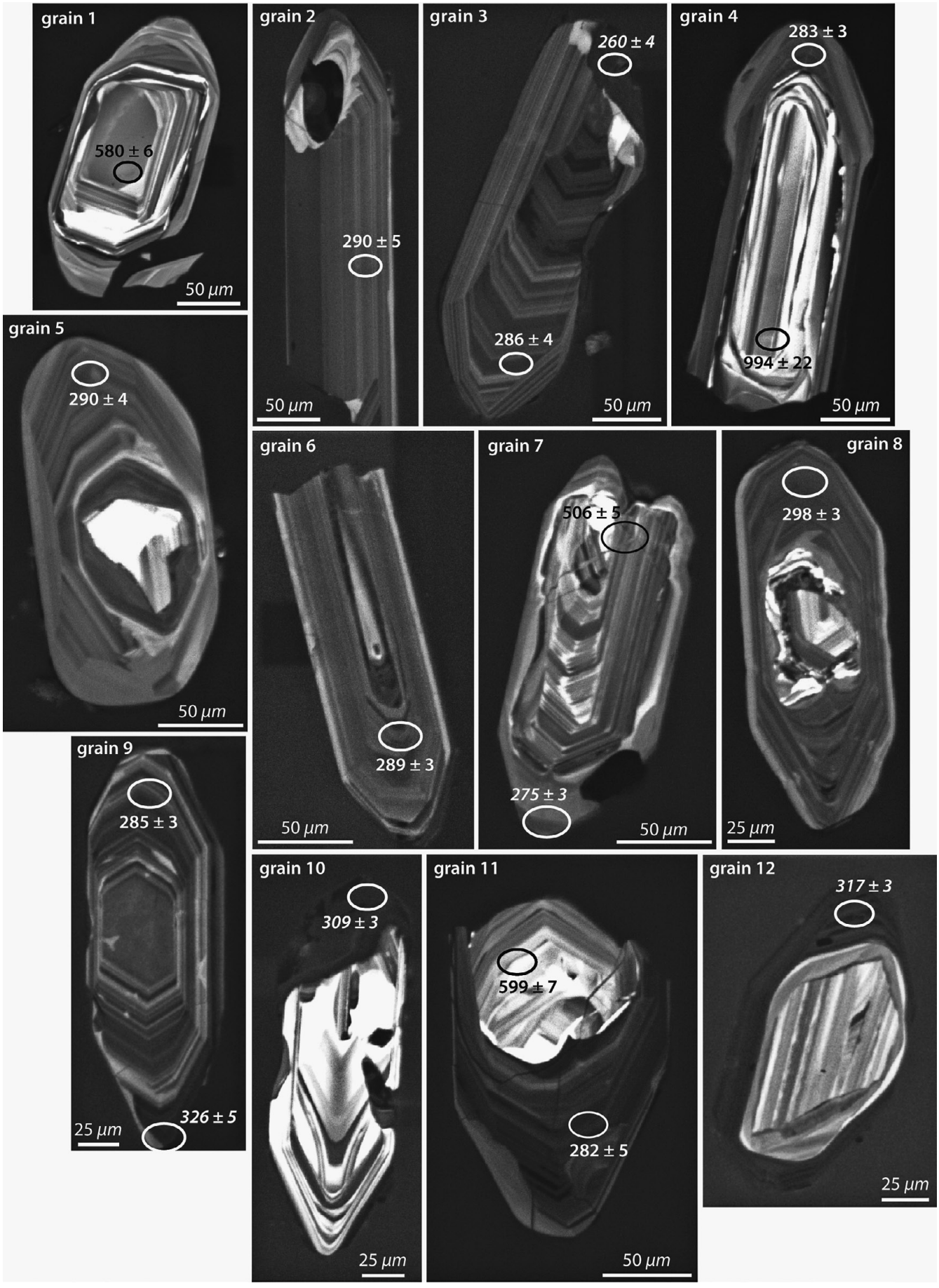

Fig. 3. SEM-CL image of zircons from sample PR12-1. Ellipses represent the spot size. The $^{206}Pb/^{238}U$ ages are reported in million years at the 1σ level of precision. The ages shown in italic are for areas with very high U (*c*. 4800–7200 ppm).

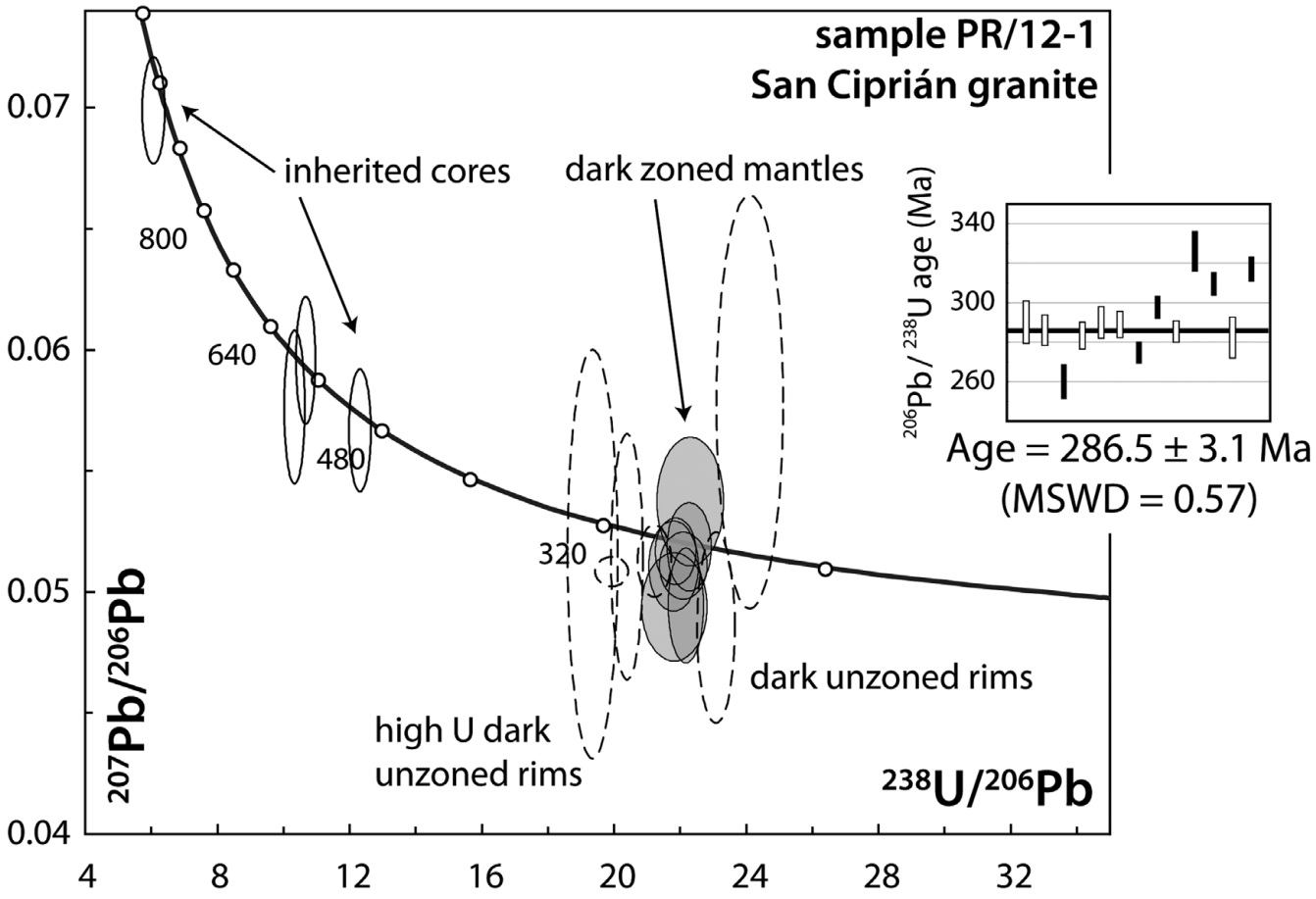

Fig. 4. PR12-1 sample results. Tera–Wasserburg and weighted average plots. Continuous-line open error ellipses are the bright oscillatory-zoned cores. Dashed-line open and continuous-line filled error ellipses are the high-U dark unzoned rims and dark-zoned mantles respectively. Data-point error ellipses are 2σ. In inset figure, white and black bars correspond to the dark-zoned mantles and dark unzoned rims respectively. Ages of dark-zoned mantles were used to calculate weighted average age.

Table 1. *U and Th contents in zircons in the San Ciprián massif*

Zircon location	Sample size	Uranium* (ppm)	SD	Thorium* (ppm)	SD	Th/U (average)	Age (Ma)
Sample DGP-09†							
Bright cores	23	350	131	126	51	0.33	Mostly Ediacaran
Dark rims	3	2352	743	77	44	0.03	287
Sample PR12-1							
Bright cores	4	404	215	157	62	0.31‡	Mostly Ediacaran
Dark rims	8	1524	587	59	32	0.05	287
Unzoned tips	5	4228	2614	68	55	0.02	–

*Average values.
†Data from table 5 of Lopez-Sanchez *et al*. (2015).
‡Only cores with Ediacaran ages were taken into account.

cores were included in the analysis, the whole-rock Th/U ratios are not representative of the actual Th/U ratio of the 287 Ma magma. Assuming an average Th/U ratio in the inner cores of *c*. 0.3 (Fig. 5a), the whole-rock Th/U ratio of the magma would be slightly higher than the measured values. Comparing U and Th whole-rock content with data for other igneous rocks (table 2 of Kirkland *et al*. 2015), the San Ciprián massif is relatively enriched in uranium and somewhat depleted in thorium. The granite dyke is remarkably richer in U than the coarse-grained facies; indeed, it has more than twice the uranium content of the coarse-grained facies, but similar Th/U ratios in zircons (Table 3).

Taking the zircon and whole-rock data obtained, a comparison was established between the U and Th zircon/whole-rock ratios in the San Ciprián massif and the data obtained for other granites provided in table 4 of Kirkland *et al*. (2015). Table 5 indicates that the U content of zircon mantles with respect to whole-rock U content is 5.1–7.2 times higher than the average in granites. In contrast, the Th content is roughly similar to those values expected considering the reference values. The very low average $Th_{(zircon/whole\text{-}rock)}/U_{(zircon/whole\text{-}rock)}$ ratio obtained in both samples (Table 5) points to a fractionation process during the crystallization of the dark-zoned mantles and, interestingly, to a low temperature of crystallization (compare fig. 10a of Kirkland *et al*. 2015). The latter could explain the abundance of inherited zircon grains (which become cores) within the San Ciprián massif. This working hypothesis may require further testing with complementary techniques (e.g. Ti-in-zircon thermometer), as other factors, such as the presence of large and good-quality original zircon crystals, or the degree of Zr saturation during the magma fractionation, may have contributed in equal measure.

Table 2. *SHRIMP U–Th–Pb data (sample PR12-1) for zircon from the San Ciprián granite*

Sample*	Location†	Measured $^{204}Pb/^{206}Pb$	Measured $^{207}Pb/^{206}Pb$	% common ^{206}Pb	U (ppm)	Th/U	Age (Ma)		$^{238}U/^{206}Pb$	Error§ (%)	$^{207}Pb/^{206}Pb$¶	Error§ (%)
							$^{206}Pb/^{238}U$‡	Error§ (%)				
PR12-1-4.2	ozc	0.000019	0.0701	−0.26	244	0.884	994	22	6.02	2.3	0.0698	1.3
PR12-1-11.2	ozc	0.000117	0.0594	−0.05	288	0.248	599	7	10.29	1.3	0.0577	2.2
PR12-1-1.1	ozc	0.000070	0.0607	0.16	366	0.426	580	6	10.62	1.1	0.0597	1.8
PR12-1-7.2	ozc	0.000199	0.0597	0.29	717	0.259	506	5	12.26	1.1	0.0568	1.8
PR12-1-8.1	dkzr	0.000056	0.0523	0.00	1808	0.043	298	3	21.19	1.0	0.0515	1.2
PR12-1-5.1	dkzr	0.000018	0.0515	−0.07	951	0.123	290	4	21.76	1.4	0.0513	1.5
PR12-1-2.1	dkzr	0.000062	0.0505	−0.20	934	0.057	290	5	21.79	1.9	0.0496	1.8
PR12-1-6.1	dkzr	0.000065	0.0528	0.09	2426	0.014	289	3	21.81	1.2	0.0519	1.1
PR12-1-3.1	dkzr	0.000011	0.0514	−0.07	1464	0.031	286	4	22.05	1.4	0.0513	1.1
PR12-1-9.1	dkzr	0.000290	0.0539	0.24	1791	0.047	285	3	22.16	1.0	0.0497	1.9
PR12-1-4.1	dkzr	0.000000	0.0520	0.01	801	0.021	283	3	22.25	1.2	0.052	1.4
PR12-1-11.1	dkzr	0.000412	0.0599	1.00	2018	0.021	282	5	22.27	1.8	0.0539	2.0
PR12-1-9.2	uzt	0.000812	0.0636	1.33	4874	0.030	326	5	19.32	1.6	0.0517	6.6
PR12-1-12.1	uzt	0.000025	0.0514	−0.16	7166	0.014	317	3	19.89	1.0	0.051	0.5
PR12-1-10.1	uzt	0.003305	0.1001	5.92	5984	0.001	309	3	20.36	1.0	0.0516	4.0
PR12-1-7.1	uzt	0.000429	0.0551	0.41	867	0.043	275	3	23.05	1.0	0.0488	3.3
PR12-1-3.2	uzt	0.003261	0.1054	6.73	2251	0.022	260	4	24.08	1.7	0.0579	5.9

*Samples analysed December 2013 on the USGS–Stanford SHRIMP-RG.
†Abbreviations: ozc, oscillatory-zoned core; dkzr, dark-zoned rim; uzt, unzoned tip.
‡$^{206}Pb/^{238}U$ ages corrected for common Pb using the ^{207}Pb-correction method. Decay constants from Steiger & Jäger (1977).
§1σ errors.
¶Radiogenic ratios, corrected for common Pb using the ^{204}Pb-correction method, based on the Stacey & Kramers (1975) model.

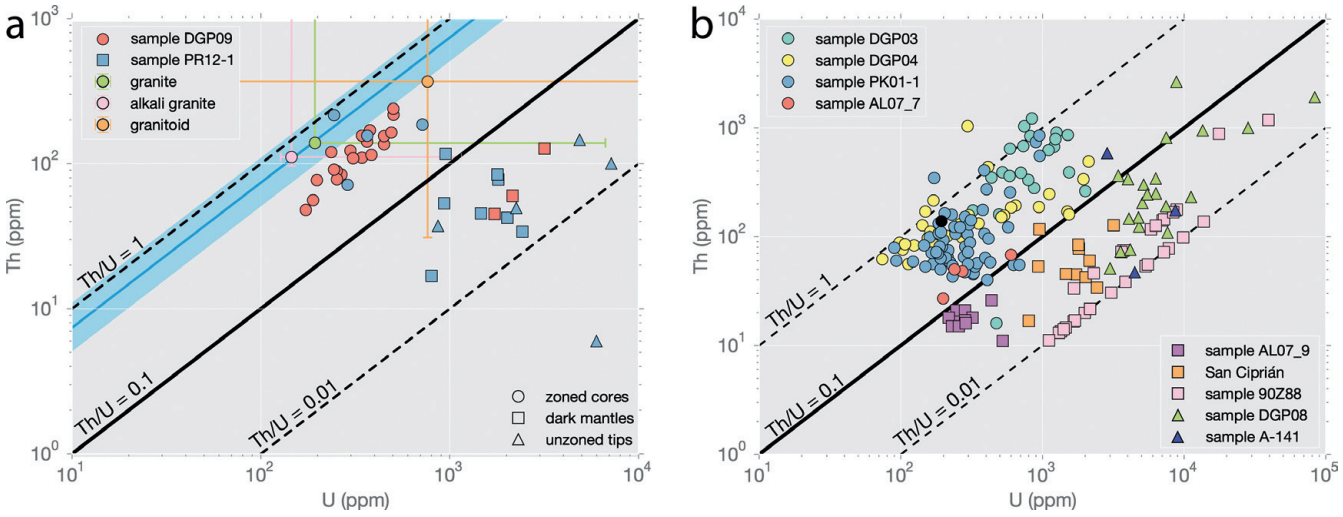

Fig. 5. (**a**) Th v. U content plot of the zircon domains from the studied samples. Values of Th and U in igneous zircons belonging to various granitoids, granites and alkali granites taken from Belousova *et al*. (2002) (in orange) and Kirkland *et al*. (2015) (in green and pink) are represented for reference. The blue shading area represents the most typical values (the interquartile range) of Th/U in zircon indicated in Figure 1a. (**b**) Comparison of Th v. U content in igneous zircon from various peraluminous granitoids (details of samples are given in Table 4). The black dot, used as reference frame, is the Tukey's biweight robust mean of all values obtained in granites by Kirkland *et al*. (2015).

The different partitioning behaviour of thorium and uranium between zircon and the magma might indicate that the coexisting minerals have to play a role in the anomalous Th/U ratios obtained. In low-Ca peraluminous granites, such as the San Ciprián massif, the fraction of Th and U residing within the major minerals is very low (<5 wt%) (Bea 1996). Therefore, REE–Y–Th–U-rich accessory minerals are likely candidates to enrich or deplete the zircon in U and Th, respectively. In particular, monazite, which yields similar crystallization ages to those found in the dark-zoned mantles, and apatite are reasonable candidates for Th depletion in the magma and consequently in zircon. However, the value of $Th_{(zircon/whole\text{-}rock)}$ obtained indicates that the Th depletion is similar to that found in other granites, even in the case of the granite dyke (DGP-09) where there is a relatively small enrichment (Table 5). This value suggests that the contemporaneous crystallization of Th-rich accessory minerals such as monazite and, perhaps, apatite does not lead to an anomalous depletion in Th during the magma fractionation. However, the crystallization of these Th-rich accessories together with the reported absence of typical U-rich accessory minerals in low-Ca peraluminous granites (xenotime, uraninite and betafite–pyrochlore; Bea 1996), could have prevented the enrichment of Th in the magma whereas it increased the U content during the fractionation process, explaining the very low Th/U ratios measured in zircon rims. This working hypothesis requires further work to confirm the absence of U-rich accessory minerals using systematic imaging by SEM–backscattered detector or mapping by X-ray diffraction in thin sections, techniques that were not used in previous studies in the area.

Table 3. *Whole-rock major and trace elements from the San Ciprián massif*

Sample	XRF, major elements (wt%)											
	SiO_2	Al_2O_3	TFe_2O_3	MnO	MgO	CaO	Na_2O	K_2O	TiO_2	P_2O_5	LOI	Total
DGP-09	72.26	14.32	0.96	0.02	0.41	0.70	2.36	7.85	0.12	0.07	0.90	99.98
PR12-1	71.81	14.46	1.17	0.02	0.27	0.49	2.78	5.14	0.13	0.32	2.48	99.08

Element	XRF, trace elements (ppm)			FUS-MS, trace elements (ppm)		
	Detection limit	DGP-09	PR12-1	Detection limit	DGP-09	PR12-1
V	3	10.2	5.9	5	7	bd
Cr	2	20.9	14.1	20	bd	50
Co	3	30.6	49	1	28	40
Ni	2	2.1	2.4	20	bd	bd
Cu	2	bd	9.3	10	bd	bd
Zn	1	22.6	47.4	30	30	50
Ga	1	14.2	20.1	1	16	21
Ge	1	bd	bd	0.5	1.2	1.4
As	3	bd	4.5	5	bd	bd
Br	1	1.1	8.1			
Rb	1	271.4	322.7	1	276	326
Sr	1	114.4	41.6	2	118	42
Y	1	6.6	12.4	0.5	6.5	12.8
Zr	1	70.5	75	1	74	66
Nb	1	6	20	0.2	4.6	15.2
Mo	1	bd	bd	2	bd	4
Ag	3	3.2	bd	0.5	bd	bd
Cd	3	bd	3.4			
In				0.1	bd	0.1
Sn	2	5.8	18.5	1	7	19
Sb	3	bd	bd	0.2	bd	bd
Te	3	5.2	3.9			
I	4	bd	30.9			
Cs	5	9.3	40.4	0.1	7	33.3
Ba	8	961.2	184.8	3	1010	205
La	8	13.6	11.7	0.05	14.9	13
Ce	7	22.7	26.2	0.05	26.9	25.1
Pr	11	bd	bd	0.01	3.26	3.3
Nd	4	10.5	11.9	0.05	11.7	11.9
Sm	5	bd	bd	0.01	2.51	3.06
Eu				0.005	0.551	0.324
Gd	5	bd	bd	0.01	1.75	2.71
Tb				0.01	0.27	0.44
Dy				0.01	1.48	2.52
Ho				0.01	0.26	0.45
Er				0.01	0.68	1.25
Tm				0.005	0.097	0.179
Yb	4	bd	bd	0.01	0.62	1.17
Lu				0.002	0.093	0.093
Hf	3	4.5	3.8	0.1	2.3	2.4
Ta	3	bd	bd	0.01	0.7	3.32
W	2	199.4	203	0.5	232	228
Tl	2	2.1	bd	0.05	1.65	1.83
Pb	2	47.8	38.6	5	38	26
Bi	1	bd	bd	0.1	bd	0.3
Th	2	7.6	9.1	0.05	8.11	10.1
U	1	8.6	5	0.01	10.5	4.86
Th/U		0.88	1.82		0.77	2.08

LOI, loss on ignition; bd, below detection limit.

Our work has shown that, in contrast to what was previously established elsewhere, Th/U ratios are not completely reliable indicators of zircon growth environment, whether magmatic of metamorphic. The San Ciprián massif is a granitic intrusion that is very well constrained geologically, with the potential to become a reference locality for further study of high-U low-Th/U zircon magmatic overgrowths and the processes forming zircon mantles at high magnification. Our contribution also highlights the importance of Th and U partitioning between zircon and other REE–Y–Th–U-rich accessory minerals, as it remains a challenge in understanding the geochemistry of high-grade rocks.

Table 4. *Details of samples used in Figure 4*

Sample	Granite/place	Granite type	Zircon Th/U mean	Zircon domain	Reference
PK01-1	Pikang granite/Lhasa terrane, Himalaya	Strongly peraluminous granite	0.43	Rims and cores	Zhu *et al*. (2009)
AL07_7	Åreskutan Mt./Seve nappe, Caledonian orogeny	Leucogranite	0.15	Rims and cores	Ladenberger *et al*. (2014)
AL07_9	Åreskutan Mt./Seve nappe, Caledonian orogeny	Leucogranite	0.06	Zircon rims	
90Z88	Torrox gneiss/Alpujárride nappe complex, Betic cordilleras, SE Spain	Andalusite-bearing orthogneiss; biotite granite	0.02	Zircon rims	Zeck & Whitehouse (1999)
DGP-03	Vivero monzogranite/Iberian Variscan massif, Galicia, NW Spain	Slightly peraluminous monzogranite	0.65	Rims and cores	Lopez-Sanchez *et al*. (2015)
DGP-04	Penedo Gordo granite/Iberian Variscan massif, Galicia, NW Spain	Strongly peraluminous low-Ca granite	0.61	Rims and cores	
DGP-08	Granite dykes, Sarria massif/Iberian Variscan massif, Galicia, NW Spain	Strongly peraluminous leucogranite	0.05		
A-141	Makalu leucogranite/High Himalayan unit, Himalaya	Two-mica leucogranite	0.20/0.02/0.01*		Schärer (1984)

*Schärer separated three groups of zircons based on their morphologies.

Table 5. *Zircon/whole-rock ratios for magmatic overgrows in the San Ciprián massif*

Sample	$U_{(zircon/whole\text{-}rock)}$	U enrichment/ depletion factor*	$Th_{(zircon/whole\text{-}rock)}$	Th enrichment/ depletion factor*	$Th/U_{(zircon)}$	$Th/U_{(whole\text{-}rock)}$	$Th_{(zircon/whole\text{-}rock)}/U_{(zircon/whole\text{-}rock)}$
DGP-09	224.00	5.14	9.49	1.30	0.03	≥0.77	0.04
PR12-1	313.58	7.20	5.84	0.80	0.05	≥2.08	0.02

*Relative element enrichment or depletion with respect to the average zircon/rock values reported in granites from table 4 of Kirkland *et al*. (2015).

Acknowledgements and Funding

This work was funded by the Spanish Ministry of Science and Innovation (grant numbers CGL2006-08822, CGL2006-09509, CGL2010-14890 and CGL2014-53388-P). M.A.L.-S. acknowledges a Severo Ochoa predoctoral fellowship (BP07-120) funded by the Asturian Regional Government (Spain). Reviews of earlier versions of the paper by J. Vazquez and two anonymous reviewers focused our thinking and improved this contribution.

Scientific editing by John MacDonald

References

Ahrens, L.H., Cherry, R.D. & Erlank, A.J. 1967. Observations on the Th–U relationship in zircons from granitic rocks and from kimberlites. *Geochimica et Cosmochimica Acta*, **31**, 2379–2387, http://dx.doi.org/10.1016/0016-7037(67)90009-9.

Bastida, F., Marcos, A. *et al*. 1984. *Mapa Geológico de España e. 1:200.000. Hoja nº 1 (La Coruña)*. Instituto Geológico y Minero de España, Madrid.

Bastida, F., Martínez-Catalán, J.R. & Pulgar, J. 1986. Structural, metamorphic and magmatic history of the Mondoñedo nappe (Hercynian belt, NW Spain). *Journal of Structural Geology*, **8**, 415–430, http://dx.doi.org/10.1016/0191-8141(86)90060-X.

Bea, F. 1996. Residence of REE, Y, Th and U in granites and crustal protoliths; implications for the chemistry of crustal melts. *Journal of Petrology*, **37**, 521–552, http://dx.doi.org/10.1093/petrology/37.3.521.

Bellido, F., Brande, J.L., Lasala, M. & Reyes, J. 1992. Consideraciones petrológicas y cronológicas sobre las rocas graníticas hercínicas de Galicia. *Cuadernos del Laborotorio Xeolóxico de Laxe*, **17**, 241–261.

Belousova, E.A., Griffin, W.L., O'Reilly, S.Y. & Fisher, N.I. 2002. Igneous zircon: trace element composition as an indicator of source rock type. *Contributions to Mineralogy and Petrology*, **143**, 602–622, http://dx.doi.org/10.1007/s00410-002-0364-7.

Black, L.P., Kamo, S.L. *et al*. 2004. Improved $^{206}Pb/^{238}U$ microprobe geochronology by the monitoring of a trace-element-related matrix effect; SHRIMP, ID-TIMS, ELA-ICP-MS and oxygen isotope documentation for a series of zircon standards. *Chemical Geology*, **205**, 115–140, http://dx.doi.org/10.1016/j.chemgeo.2004.01.003.

Capdevila, R. 1969. *Le métamorphisme régional progressif et les granites dans le segment hercynien Galice nord orientale (NW l'Espagne)*. PhD thesis, Université de Montpellier.

Claiborne, L., Miller, C. & Wooden, K. 2010. Trace element composition of igneous zircon: A thermal and compositional record of the accumulation and evolution of a large silicic batholith, Spirit Mountain, Nevada. *Contributions to Mineralogy and Petrology*, **160**, 511–531, http://dx.doi.org/10.1007/s00410-010-0491-5.

Dallmeyer, R.D., Martínez-Catalán, J.R. *et al*. 1997. Diachronous Variscan tectonothermal activity in the NW Iberian Massif : Evidence from $^{40}Ar/^{39}Ar$ dating of regional fabrics. *Tectonophysics*, **277**, 307–337, http://dx.doi.org/10.1016/S0040-1951(97)00035-8.

Farias, P., Gallastegui, G. *et al*. 1987. Aportaciones al conocimiento de la litoestratigrafía y estructura de Galicia Central. *Memórias da Facultade de Ciências, Universidade do Porto*, **1**, 411–431.

Fernández-Suárez, J., Dunning, G., Jenner, G. & Gutiérrez-Alonso, G. 2000. Variscan collisional magmatism and deformation in NW Iberia: constraints from U–Pb geochronology of granitoids. *Journal of the Geological Society, London*, **157**, 565–576, http://dx.doi.org/10.1144/jgs.157.3.565.

Ferrus-Piñol, B. 1994. Estructura de la cuenca de As Pontes. *Cuadernos del Laborotorio Xeolóxico de Laxe*, **19**, 73–89.

Galán, G. 1987. *Las rocas graníticas del macizo de Vivero en el sector norte (Lugo, NO de España)*. Corpus Geologicum Gallaeciae Segunda, Serie II, **3**.

Galán, G., Pin, C. & Duthou, J. 1996. Sr–Nd isotopic record of multi-stage interactions between mantle-derived magmas and crustal components in a collision context—the ultramafic–granitoid association from Vivero (Hercynian belt, NW Spain). *Chemical Geology*, **131**, 67–91, http://dx.doi.org/10.1016/0009-2541(96)00027-7.

Harley, S.L. & Kelly, N.M. 2007. Zircon tiny but timely. *Elements*, **3**, 13–18, http://dx.doi.org/10.2113/gselements.3.1.13.

Harley, S.L., Kelly, N.M. & Möller, A. 2007. Zircon behaviour and the thermal histories of mountain chains. *Elements*, **3**, 25–30, http://dx.doi.org/10.2113/gselements.3.1.25.

Hokada, T. & Harley, S.L. 2004. Zircon growth in UHT leucosome: constraints from zircon–garnet rare earth elements (REE) relations in Napier Complex, East Antarctica. *Journal of Mineralogical and Petrological Sciences*, **99**, 180–190, http://dx.doi.org/10.2465/jmps.99.180.

Hoskin, P.W.O. & Black, L.P. 2000. Metamorphic zircon formation by solid-state recrystallization of protolith igneous zircon. *Journal of Metamorphic Geology*, **18**, 423–439, http://dx.doi.org/10.1046/j.1525-1314.2000.00266.x.

Huertas, A., Parés, J.M., Cabrera, L., Ferrús, B. & Sáez, A. 1997. Magnetocronología de las sucesiones cenozoicas de la cuenca de As Pontes (La Coruña, Noroeste de España). *Acta Geologica Hispanica*, **32**, 127–145.

Ireland, T.R. 1995. Ion microprobe mass spectrometry: Techniques and applications in cosmochemistry, geochemistry, and geochronology. *In*: Hyman, M. & Rowe, M. (eds) *Advances in Analytical Geochemistry, 2*. JAI Press, Greenwich, CT, 1–118.

Julivert, M., Fontbote, J., Ribeiro, A. & Conde, I. 1972. *Mapa tectónico de la Península Ibérica y Baleares*. Instituto Geológico y Minero de España, Madrid, 246–265.

Kelly, N.M. & Harley, S.L. 2005. An integrated microtextural and chemical approach to zircon geochronology: Refining the Archaean history of the Napier Complex, east Antarctica. *Contributions to Mineralogy and Petrology*, **149**, 57–84, http://dx.doi.org/10.1007/s00410-004-0635-6.

Kirkland, C.L., Smithies, R.H. *et al*. 2015. Zircon Th/U ratios in magmatic environs. *Lithos*, **212–215**, 397–414, http://dx.doi.org/10.1016/j.lithos.2014.11.021.

Ladenberger, A., Be'eri-shlevin, Y. *et al*. 2014. Tectonometamorphic evolution of the Åreskutan Nappe—Caledonian history revealed by SIMS U–Pb zircon geochronology. *In*: Corfu, F., Gasser, D. & Chew, D.M. (eds) *New Perspectives on the Caledonides of Scandinavia and Related Areas*. Geological Society, London, Special Publications, **390**, 337–368, http://dx.doi.org/10.1144/SP390.10.

Lopez-Sanchez, M.A. 2013. *Análisis tectónico de la Falla de Vivero (Galicia, NO de España)*. PhD thesis, Universidad de Oviedo.

Lopez-Sanchez, M.A., Marcos, A. *et al*. 2015. Setting new constraints on the age of crustal-scale extensional shear zone (Vivero fault): Implications for the evolution of Variscan orogeny in the Iberian massif. *International Journal of Earth Sciences*, **104**, 927–962, http://dx.doi.org/10.1007/s00531-014-1119-1.

Lotze, F. 1945. Zur Gliederung der Varisziden der Iberischen Meseta. *Geotektonische Forschungen*, **6**, 78–92.

Ludwig, K.R. 2009. *SQUID 2: A User's Manual, rev. 12 Apr, 2009*. Berkeley Geochronological Centre Special Publications, **5**.

Ludwig, K.R. 2012. *Isoplot 3.75—A geochronological toolkit for Microsoft Excel*. Berkeley Geochronology Center Special Publications, **5**.

Marcos, A. 2013. Un nuevo mapa geológico de la parte septentrional del Domo de Lugo (Galicia oriental, NO de España): Implicaciones sobre la estratigrafía, estructura y evolución tectónica del Manto de Mondoñedo. *Trabajos de Geología*, **33**, 171–200.

Martínez, F.J., Carreras, J., Arboleya, M.L. & Dietsch, C. 1996. Structural and metamorphic evidence of local extension along the Vivero fault coeval with bulk crustal shortening in the Variscan chain (NW Spain). *Journal of Structural Geology*, **18**, 61–73, http://dx.doi.org/10.1016/0191-8141(95)00080-W.

Martínez-Catalán, J.R. 1985. *Estratigrafía y estructura del Domo de Lugo (Sector Oeste de la Zona Asturoccidental-leonesa*. Corpus Geologicum Gallaeciae Segunda, Serie II, **2**.

Möller, A., O'Brien, P.J., Kennedy, A. & Kröner, A. 2003. Linking growth episodes of zircon and metamorphic textures to zircon chemistry: An example from the ultrahigh-temperature granulites of Rogaland (SW Norway). *In*: Vance, D., Müller, W. & Villa, I.M. (eds) *Geochronology: Linking the Isotopic Record with Petrology and Textures*. Geological Society, London, Special Publications, **220**, 65–81, http://dx.doi.org/10.1144/GSL.SP.2003.220.01.04.

Pidgeon, R.T. 1992. Recrystallisation of oscillatory zoned zircon: Some geochronological and petrological implications. *Contributions to Mineralogy and Petrology*, **110**, 463–472, http://dx.doi.org/10.1007/BF00344081.

Rubatto, D. 2002. Zircon trace element geochemistry: Partitioning with garnet and the link between U–Pb ages and metamorphism. *Chemical Geology*, **184**, 123–138, http://dx.doi.org/10.1016/S0009-2541(01)00355-2.

Schaltegger, U., Fanning, C.M. *et al*. 1999. Growth, annealing and recrystallization of zircon and preservation of monazite in high-grade metamorphism: Conventional and *in-situ* U–Pb isotope, cathodoluminescence and microchemical evidence. *Contributions to Mineralogy and Petrology*, **134**, 186–201, http://dx.doi.org/10.1007/s004100050478.

Schärer, U. 1984. The effect of initial ^{230}Th disequilibrium on young U–Pb ages: The Makalu case, Himalaya. *Earth and Planetary Science Letters*, **67**, 191–204, http://dx.doi.org/10.1016/0012-821X(84)90114-6.

Sláma, J., Kosler, J. *et al*. 2008. Plešovice zircon—A new natural reference material for U–Pb and Hf isotopic microanalysis. *Chemical Geology*, **249**, 1–35, http://dx.doi.org/10.1016/j.chemgeo.2007.11.005.

Stacey, J. & Kramers, J. 1975. Approximation of terrestrial lead isotope evolution by a two-stage model. *Earth and Planetary Science Letters*, **26**, 207–221, http://dx.doi.org/10.1016/0012-821X(75)90088-6.

Steiger, R.H. & Jäger, E. 1977. Subcommission on geochronology: Convention on the use of decay constants in geo- and cosmochronology. *Earth and Planetary Science Letters*, **36**, 359–362, http://dx.doi.org/10.1016/0012-821X(77)90060-7.

Vavra, G., Schmid, R. & Gebauer, D. 1999. Internal morphology, habit and U–Th–Pb microanalysis of amphibolite-to-granulite facies zircons: Geochronology of the Ivrea Zone (Southern Alps). *Contributions to Mineralogy and Petrology*, **134**, 380–404, http://dx.doi.org/10.1007/s004100050492.

Wang, X., Griffin, W.L. *et al*. 2011. U and Th contents and Th/U ratios of zircon in felsic and mafic magmatic rocks: Improved zircon–melt distribution coefficients. *Acta Geologica Sinica*, **85**, 164–174, http://dx.doi.org/10.1111/j.1755-6724.2011.00387.x.

Watson, E.B. 1996. Surface enrichment and trace-element uptake during crystal growth. *Geochimica et Cosmochimica Acta*, **60**, 5013–5020, http://dx.doi.org/10.1016/S0016-7037(96)00299-2.

Watson, E.B. & Harrison, T.M. 1983. Zircon saturation revisited: Temperature and composition effects in a variety of crustal magma types. *Earth and Planetary Science Letters*, **64**, 295–304, http://dx.doi.org/10.1016/0012-821X(83)90211-X.

White, L.T. & Ireland, T.R. 2012. High-uranium matrix effect in zircon and its implications for SHRIMP U–Pb age determinations. *Chemical Geology*, **306–307**, 78–91.

Williams, I.S. 1998. U–Th–Pb geochronology by ion microprobe. *In*: McKibben, M.A., Shanks, W.C., III & Ridley, W.I. (eds) *Applications of microanalytical techniques to understanding mineralizing processes*. Reviews of Economic Geology, **7**, 1–35.

Williams, I.S. & Claesson, S. 1987. Isotopic evidence for the Precambrian provenance and Caledonian metamorphism of high grade paragneisses from the Seve Nappes, Scandinavian Caledonides. *Contributions to Mineralogy and Petrology*, **97**, 205–217, http://dx.doi.org/10.1007/BF00371240.

Williams, I.S. & Hergt, J.M. 2000. U–Pb dating of Tasmanian dolerites: A cautionary tale of SHRIMP analysis of high-U zircon. *In*: Woodhead, J.D., Hergt, J.M. & Noble, W.P. (eds) *Beyond 2000: New Frontiers in Isotope Geoscience: Lorne. Abstract Proceedings*, University of Melbourne, Victoria, Australia, 185–188.

Zeck, H.P. & Whitehouse, M.J. 1999. Hercynian, Pan-African, Proterozoic and Archean ion-microprobe zircon ages for a Betic–Rif core complex, Alpine belt, W Mediterranean—consequences for its *P–T–t* path. *Contributions to Mineralogy and Petrology*, **134**, 134–149, http://dx.doi.org/10.1007/s004100050474.

Zhu, D.C., Mo, X.X. *et al*. 2009. Zircon U–Pb dating and *in situ* Hf isotopic analysis of Permian peraluminous granite in the Lhasa terrane, southern Tibet: implications for the Permian collisional orogeny and paleogeography. *Tectonophysics*, **469**, 48–60, http://dx.doi.org/10.1016/j.tecto.2009.01.017.